Romanian Reports in Physics, Vol. 59, No. 3, P. 773–790, 2007

ANALYSIS OF HIGH N_S - MULTIPLICITY EVENTS PRODUCED IN RELATIVISTIC HEAVY ION COLLISIONS AT 4.5A GeV/c

M. TARIQ[+], M. Ayaz AHMAD[*], Shafiq AHMAD[*] and M. ZAFAR[*]

+Department of Physics, Govt. Raza P.G.College, Rampur-244901, U. P. India.
** Physics Department, Aligarh Muslim University, Aligarh-202002, India*
E- mail: sahmad2004amu@yahoo.co.in

(Received November 30, 2005)

Abstract. In the present work we report some results based on the study of mean multiplicities, multiplicity distributions of various charged secondaries and some of their correlations along with angular distributions of the target fragments produced in the central collisions of ^{28}Si and ^{12}C nuclei at 4.5A GeV/c with nuclear emulsion. A new criteria for selecting most central collision events having high N_S-multiplicity events has been proposed and termed as the events of total destruction. An attempt has been made to see the dependence of degree of centrality on the mass of projectile in nuclear collision. Finally, the increase in the height of centroid of normalized pseudorapidity distributions could be explained in terms of geometry of the collision.

Key words: relativistic heavy ion collisions; nuclear emulsion; forward to backward ratio.
PACS: 25.75. -q, 29.40Rg

1. INTRODUCTION

The main concern of high-energy physics is the study of fundamental particles and their interactions. The interaction between elementary particles and nuclei is so important that one might even say that the problem of elementary particles is today the problem of physics. Moreover, the relativistic heavy ion collisions has opened up an entirely new region in the exploration of various cosmological and astrophysical problems, in addition to the physics of quarks, elementary particles and nuclei. The primary motivation to produce interactions of heavier and heavier beam nuclei at increasing energies is to obtain an energy density of a magnitude over sufficiently large volume so that the elementary particles loose their identity to form a Quark-Gluon Plasma (QGP) [1-3] and a thermal equilibrium is achieved. It may be presumed that direct or indirect signal of QGP-formation could be obtained from the plasma itself (through γ-rays, leptons pairs, etc.) as well as from hadronization (through fluctuations and correlations due

to local instabilities and different pairing of quarks). The nuclear phenomenon of multiparticle production in central collision domain is expected to provide substantial information about the nuclear matter compressed to several times its normal density.

We have already studied the normalized single-particle exclusive distributions for various high N_S-multiplicity events of ^{28}Si-Em and ^{12}C-Em interactions at 4.5A GeV/c. The result has been reported [4]. It was realized that an extension of the work is must. Similar analysis was also done by N. N. Abd Allah et al [5]. They have studied the dependence of various characteristics of relativistic charged particles on their multiplicity by dividing the entire data into different ensembles of N_S-bins. Apart from these, the analysis of high N_S-multiplicity events produced in relativistic nuclear collisions is still important and relevant for studying the multiparticle production in such collisions with small impact parameter. As in collisions of hadrons with nucleons and nuclei, a large part of the total cross–section for nucleus–nucleus interactions at high energies is due to multiple productions of particles. Thus, a deep inelastic collision is expected to give rise large number of relativistic charged particles in the final state of the reaction. Based on the above considerations it seems to be genuine to assume the multiplicity of relativistic charged shower particle N_S, in an event as a vital parameter to study the degree of centrality i.e. average impact parameter. It will be worth mentioning at this juncture that this method allows the admixture of quasi-central collision events of few AgBr-nuclei to the most central collision events of all H, CNO as well as rest of AgBr-nuclei in the final ensemble. A modest attempt has been made in the present study to unearth the dynamics of multiparticle production in the high N_S-events and to see the dependence of degree of centrality beside its effect on the projectile mass. The results presented in this paper include the study of mean multiplicities, multiplicity distributions of various charged secondaries and some of their inter-correlations along with angular distributions of the target fragments emanating from the disintegration of emulsion nuclei. Moreover, the normalized single particle exclusive (pseudorapidity) distributions of the relativistic charged shower particles produced in the event of interest have also been studied. The data comprising of 701 ^{28}Si-Em interactions and 844 ^{12}C-Em interactions at 4.5A GeV/c have been utilized in the present study. The analysis of Proton-Em data at same momentum per nucleon has also been used for the purpose of comparison [6].

2. EXPERIMENTAL DETAILS

Two stacks of BR-2 emulsion exposed to 4.5A GeV/c Silicon and Carbon beams at Synchrophasotron of Joint Institute of Nuclear Research (JINR), Dubna, Russia, have been used to collect the data. The dimensions of pellicles, incident

flux of the beams, etc. are given in our publication [7]. Along the track scanning method was adopted to pick up events of interest, which was carried out using Japan made NIKON (LABOPHOT and Tc-BIOPHOT) microscopes with 40X objectives and 10X eyepieces. Some of experimental details pertaining to the present study will be discussed in the subsequent sections of this paper whereas other relevant details may be seen in our earlier publications [7-9].

2.1. CLASSIFICATION OF TRACKS

The tracks emanating from each interaction were categorized according to the commonly accepted emulsion experiment terminology, into following groups:

Black tracks (N_b). The tracks having specific ionization $g^* > 10$ ($g^* = g/g_0$, where g_0 is the Plateau ionization of relativistic singly charged particles and g is the ionization of the charged secondary) are called black tracks. This corresponds to protons of relativistic velocity β ($= v/c$) < 0.3 and range in emulsion $L < 3.0$ mm.

Grey tracks (Ng). The tracks with $1.4 \leq g^* \leq 10$ are called the grey tracks which corresponds to protons with velocity in interval $0.3 \leq \beta \leq 0.7$ and range $L \geq 3.0$ mm in emulsion. The grey tracks are associated with the recoiling protons and are assumed to be a measure of effective target thickness.

Heavily ionizing tracks (N_h). The black and grey tracks taken together are termed as heavily ionizing tracks. Thus these tracks correspond to $g^* \geq 1.4$. Their number in a star, N_h ($= N_b + N_g$) is a characteristic of the target.

The material of nuclear emulsion and liquid of bubble chamber are the examples of materials, which act as target and detector both. In this respect the role of nuclear emulsion is quite clear. In fact, as often proved in the past, owing to their continuous sensitivity, exceptional spatial resolution in 3-dimensions ~ 1 μm and 4p solid angle coverage, emulsions have perfectly suited for many pioneering works that lead insight to more refined experiments. The role played by cosmic ray events detected in nuclear emulsions in triggering new ideas and method of analysis is very well known.

As a consequence of technological advancement, various shortcomings of nuclear emulsions have been eliminated, e.g., the hybrid experiments linking emulsion with external electronic devices to select the rare or some times very rare events with a rejection factor down to $10^{-4} - 10^{-5}$ and preserving the high spatial accuracy and multitrack and multivertex discrimination, the experiments coupled with sophisticated semi-automatic/automatic scanning and measurement apparatus to overcome the biggest drawback, viz., long analysis time, the popular emulsion chambers loaded with a broad spectrum of targets with limited solid angle, etc. Beside the above mentioned merits and improvements made, some times it is very difficult rather impossible to recognize the very dipping tracks particularly grey and/or black tracks having $\theta_d > 30^\circ$.

In order to correct for any possible loss of the very dipping tracks in the experiment, only those heavily ionizing particles have been considered for average multiplicity calculations which are having $\theta_d < 30^\circ$ and a geometrical correction factor *K* which has been used earlier by other workers [10,11], is attached to each heavily ionizing particle with $\theta_d < 30^\circ$ such that

$$K = 1, \text{ when } 150^\circ \leq \theta_s \leq 30^\circ,$$

otherwise,

$$K = \pi / 2\sin^{-1}\left(\sin 30^0 / \sin\theta_s\right),$$

where $?_s$ is the space angle of the track.

The mean multiplicities of target fragments, i.e., mean multiplicities of grey and black tracks with and without weight factor/geometrical correction factor *K* will be discussed in first section results and discussions for the sake of completeness and to have justification to use the *K*, the geometrical correction factor.

Shower tracks (N_S). The tracks having $g^* < 1.4$ are taken as shower tracks ($\beta > 0.7$). Shower tracks producing particles are mostly charged pions with small admixture of charged kaons and fast protons.

2.2. IDENTIFICATION OF PROJECTILE FRAGMENTS

In a peripheral collision only a part of the projectile nucleus is directly involved in the collision. Therefore, the projectile nucleus breaks up into singly charged fragments, neutral particles and also into multiply charged fragments. During data analysis these fragments have also been grouped into doubly and multiply charged fragments based on the following criteria:

Doubly charged PFs (Z = 2). The particles having $g^* \sim 4$ with no change in ionization along a length of at least 2 cm from the interaction vertex and having an angle of emission $\theta < 4^\circ$.

Multiply charged PFs (Z ³ 3). The particles with $g^* > 6$, $\theta < 4^\circ$ and without any change in ionization along a length of at least 1 cm from the vertex have been put under the category of multiply charged PFs ($Z \geq 3$).

It is needless to mention that the above cited charged projectile fragments do not include the grey and/or black tracks producing particles since those are considered as target fragments.

The charge estimation of PFs has been done by ionization measurements and by d-ray countings. It is not possible to separate fragments of charge $Z = 1$ by these methods. However, their number has been estimated and excluded from the multiplicity of shower particles and the details may be found else where [10]. The details regarding the angular measurements and various selection criteria may be found else where [6, 10].

2.3. GROUPING OF TARGETS

The exact identification of targets in emulsion experiments is not possible since the medium of the emulsion is heterogeneous and composed of H, C, N, O, Ag and Br nuclei. However, the events with $N_h = 1$ are generally taken to be due to interactions with H ($A_T = 1$) and those having $2 = N_h = 7$ are considered to be due to interactions with CNO or light group of nuclei ($\langle A_T \rangle = 14$). Similarly, the events with $N_h = 8$ are put under the category of interactions with AgBr or heavy group of nuclei ($\langle A_T \rangle = 94$). However, the grouping of events only on the basis of N_h values does not lead to the right percentage of events of interactions due to light and heavy group of nuclei. In fact, a considerable fraction of stars with $N_h \leq 7$ are produced in the interactions with heavy group of nuclei. Therefore, we have used the criterion based on the works reported Barashenkov et al [12] and Jacobsson and Kullburg [13] for putting the events under various groups. The criterion used by us is as follows:

AgBr events:

(i) $N_h > 7$, or

(ii) $N_h \leq 7$ and at least one track with range, $R \leq 10$ μm and no track with $10 < R \leq 50$ μm;

CNO events:

(i) $2 \leq N_h \leq 7$ and no track with $R \leq 10$ μm;

H events:

(i) $N_h = 0$, or

(ii) $N_h = 1$, and no track with $R \leq 50$ μm.

3. DATA ANALYSIS

Recently, several authors have investigated the various features of particle production such as thermalization and hadronization, which are expected to be inherent in the entire rapidity space of the central collision events both in high-energy hadron-nucleus and nucleus-nucleus collisions [10, 11, 14-16]. Various criteria for selecting central collision events may be found in the literature [10, 11, 15-17]. The criteria for the selection of the events of central collision must be based on the fact that the emanating particles in relativistic nuclear interactions come from either target/projectile fragmentation and/or central/ pionic regions of the rapidity space, which are available for the multiparticle production. Thus, it is genuinely argued that the heavily ionizing tracks (N_h), produced in the interactions due to the target fragmentation may be one of the criterion for selecting the central collision events (i.e., events having $N_h = 28$). However, it limits the analyses of the events of total destruction due to only Ag Br nuclei. There is another commonly accepted method employed in emulsion experiments based on the projectile

fragmentation using the parameter Q, which is the fraction of the charge of the projectile nucleus going into fragments and defined as $Q = \sum_f Z_f$; Z_f is the charge of f^{th} kind in an event (i.e. events having Q = 0,1). This method allows the admixture of quasi-central collision events (with Q = 1) to the most central collision events (with Q = 0) in the final ensemble and suitable for comparison in the present study. In view of the above, the high N_S–multiplicity events (i.e., events having N_S = 3, N_S = 14 and N_S = 28 for Proton-Em, ^{12}C-Em and ^{28}Si-Em interactions respectively) are assumed to be the central collision events. This criterion is applied in the present experiment due to the facts that firstly, it allows the study of all emulsion nuclei, i.e., H, CNO as well as AgBr and secondly, the shower particles mainly come from the extended central region and not from the either limited fragmentation regions viz. projectile and target fragmentation regions with large and small η–values respectively. It will be worth mentioning here that the criteria for selecting the events of central collision based on high N_S-multiplicity is arbitrary. Also this method does not eliminate the quasi-central collisions of heavy nuclei (AgBr) from the final ensembles. However, the events having multiplicity of relativistic charged shower particles either equals to or greater than the twice of the mean multiplicity of relativistic charged shower particles, i.e., the events with N_S = 2 $<N_S>$ were categorized as central collision disintegrations. This could be verified from Table 1. The average multiplicity of charged shower particles in ^{28} Si-Em data for total 701interactions is 13.97 ± 0.14 and twice of it, i.e., with N_S = 28, a total 110 events (15.69%) were selected for final analysis. Similarly, in ^{12}C-Em for 844 interactions the mean multiplicity of charged shower particles is 7.27 ± 0.12. Thus, the disintegrations with N_S = 14, a total 82 (9.72%) events were included in the study. Additionally, the $<N_S>$ in Proton-Em interactions for 2576 events is reported to be 1.63 ± 0.02 and with N_S = 3, a total of 512 events (19.87%) were utilized for the study of the central collision in this paper. Beside the above, we have analyzed our data of ^{28}Si-Em and ^{12}C-Em data using the well established method based on the spectator part of projectile fragments appearing in the final state of the reaction, i.e., using the parameter Q and the findings were compared with above results. A total of 98 events (13.98%) of ^{28}Si-Em and 317 interactions (37.56%) of ^{12}C-Em data with Q = 0,1 were used.

4. EXPERIMENTAL RESULTS

4.1. MEAN MULTIPLICITY OF VARIOUS PARTICLES PRODUCED

The mean multiplicities of various target fragments, viz., grey and black tracks with and without use of a geometrical correction factor K have been determined for both ^{28}Si-Em and ^{12}C-Em data. The values of $<N_b>$ are found to be

6.90 ± 0.10 and 7.23 ± 0.09 for 701 events of ^{28}Si-Em and for 844 events of ^{12}C-Em respectively without utilizing the geometrical correction factor *K*. The values of the same parameter for the same ensembles after utilizing the geometrical correction factor K are estimated to be 5.26 ± 0.09 and 4.51 ± 0.10 respectively. The values of $<N_g>$ are 5.03 ± 0.09 and 5.42 ± 0.08 for all events of ^{28}Si-Em and for all events of ^{12}C-Em respectively without incorporating the geometrical correction factor *K*. The estimated values of $<N_g>$ after utilizing the geometrical correction factor *K* for the same ensembles are 6.33 ± 0.10 and 5.75 ± 0.11. It will be worth mentioning at this juncture that the values of mean multiplicities of black and grey tracks calculated with the help of above mentioned geometrical correction factor *K* are in agreement with the reported results [6, and references therein]. From the above estimations, it is quite clear that the values of $<N_b>$ are over estimated and the values of $<N_g>$ are under estimated in the bare measurements in comparison to the estimations involved a geometrical correction factor *K* which enables us genuinely to use the geometrical correction/weight factor *K* for estimation of mean multiplicities of various target fragments.

Table 1

Mean multiplicities of various tracks produced in nuclear collisions at 4.5A GeV/c

Kinds of Interaction	$<N_b>$	$<N_g>$	$<N_b>/<N_g>$	$<N_S>$	Ensembles	References
^{28}Si-Em	5.26 ± 0.09	6.33 ± 0.10	0.83 ± 0.019	13.97 ± 0.14	All N_S	(10)
	10.33 ± 0.31	13.48 ± 0.35	0.77 ± 0.031	36.17 ± 0.57	$N_S \geq 28$	Present work
	9.90 ± 0.65	12.15 ± 0.75	0.81 ± 0.053	33.29 ± 0.58	$Q = 0,1$	Present work
^{12}C-Em	4.51 ± 0.10	5.75 ± 0.11	0.78 ± 0.023	7.27 ± 0.12	All N_S	(10)
	9.00 ± 0.33	14.57 ± 0.42	0.62 ± 0.029	25.34 ± 0.56	$N_S \geq 14$	Present work
	10.36 ± 0.82	11.79 ± 0.52	0.88 ± 0.080	10.39 ± 0.18	$Q = 0,1$	Present work
Proton-Em	3.77 ± 0.08	2.81 ± 0.06	1.34 ± 0.040	1.63 ± 0.02	All N_S	(6)
	3.68 ± 0.08	2.47 ± 0.07	1.49 ± 0.053	3.33 ± 0.08	$N_S \geq 3$	Present work

The mean multiplicities of black, grey and shower tracks in total disintegrations using both the criteria for selecting central collision events as obtained in the present work for ^{28}Si-Em, ^{12}C-Em and Proton-Em data are listed in Table 1. From this table one may notice that the values of $<N_g>$ as well as $<N_b>$ in ^{28}Si-Em and ^{12}C-Em central collisions are almost double of the respective values of $<N_g>$ and $<N_b>$ for all events, whereas that of Proton-Em data is almost unchanged. However, the ratio $<N_b>/<N_g>$ essentially remains same for all ensembles which could be understood in term of the geometry of the collisions. The increase in the values of $<N_S>$ may be attributed to the fact that the relativistic charged shower particles come mostly from the central/pionic region of rapidity space, which is essentially enhanced in the case of complete destruction of nuclei.

Thus the nucleus-nucleus interactions could be understood in term of a superposition of a number of elementary intranuclear nucleon-nucleon collisions even in the case of central collision events.

4.2. MULTIPLICITY DISTRIBUTIONS OF DIFFERENT TRACKS

The multiplicity distributions of target fragments, i.e., grey and black tracks producing particles emitted in ^{28}Si-Em, ^{12}C-Em and Proton-Em interactions for high N_S-multiplicity events and Q = 0,1 events of ^{28}Si-Em and ^{12}C-Em are shown in Figs. 1 (a, b) and 2 (a, b) respectively. It may be seen from these figures that the distributions are essentially similar for both the ensembles of the central collisions

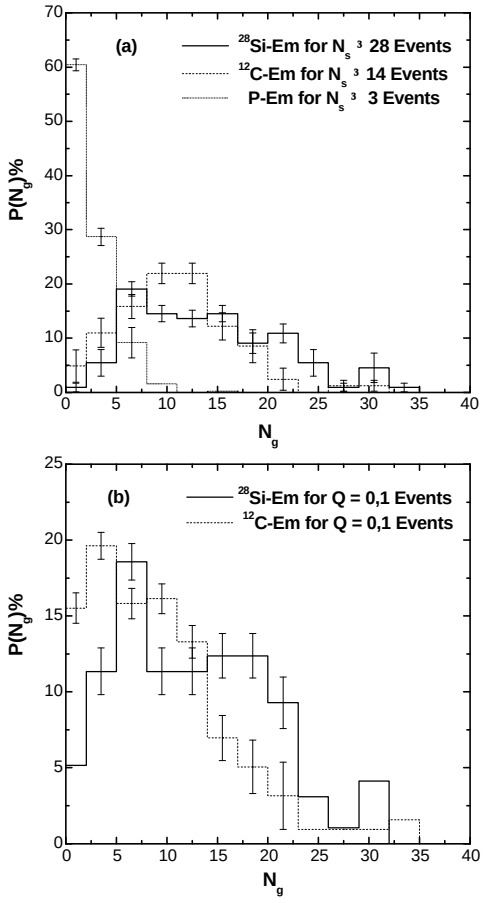

Fig. 1 – Multiplicity distributions of grey tracks: a) for $N_s \geq 28$ events of ^{28}Si-Em, $N_s \geq 14$ events of ^{12}C-Em and Ns ≥ 3 events of P-Em; b) for Q = 0,1 ensembles of ^{28}Si-Em and ^{12}C-Em interactions at 4.5A GeV/c.

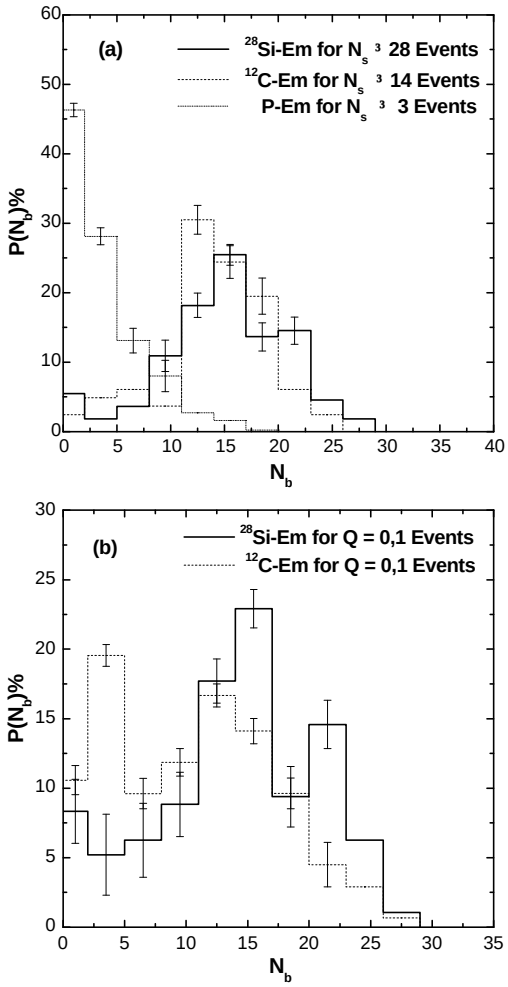

Fig. 2 – Multiplicity distributions of black tracks: a) for $N_s \geq 28$ events of ^{28}Si-Em, $N_s \geq 14$ events of ^{12}C-Em and Ns ≥ 3 events of P-Em; b) for $Q = 0,1$ ensembles of ^{28}Si-Em and ^{12}C-Em interactions at 4.5A GeV/c.

in nucleus-nucleus interactions and differ in the case of Proton-Em data. It is noticed from the figures that in nucleus-nucleus collisions majority of the events are from the larger N_g- and N_b-multiplicity events as the peaks are not at the lower values of the respective tracks, whereas in Proton-Em interactions peaks are at lower values of the respective tracks thus contributes respectively more at lower values. A projectile mass dependence could be seen in these plots. The multiplicity distributions of heavily ionizing tracks produced in the central collisions for the same ensembles of the data are shown in Fig. 3 (a, b). A strong projectile mass dependence could be recorded in these graphs. On looking these plots, it may be

visualized that in nucleus-nucleus interactions, most of the events of central collisions are high N_h-multiplicity interactions, which suggests that the high N_h-multiplicity events may also be regarded as events of total destruction. In Proton-Em interactions the inference from these plots is however not same.

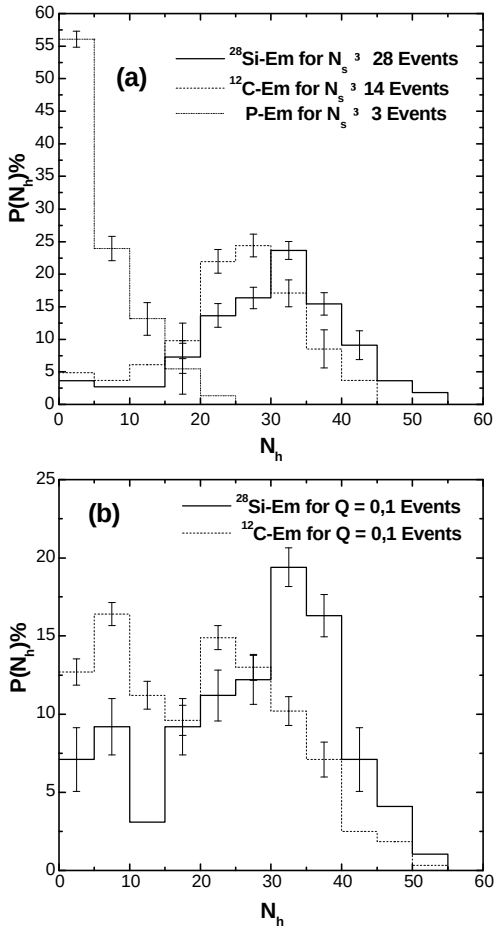

Fig. 3 – Multiplicity distributions of heavily ionizing tracks: a) for $N_s \geq 28$ events of ^{28}Si-Em, $N_s \geq 14$ events of ^{12}C-Em and $N_s \geq 3$ events of P-Em; b) for $Q = 0,1$ ensembles of ^{28}Si-Em and ^{12}C-Em interactions at 4.5A GeV/c.

4.3. MULTIPLICITY CORRELATIONS

Multiplicity correlations of the type $<N_i\ (N_j)>$, where N_i, $N_j = N_g$, N_b, N_h and N_S (with i ? j) have been widely studied with various projectiles and target combinations. We present here some of the inter-correlations of similar kind for the

central collision ensembles (with high N_S – multiplicity events) for three different projectiles, viz., Silicon-28, Carbon-12 and Proton beam at the same per particle incident momenta. The experimental results exhibiting the dependence of (a) $\langle N_b \rangle$ on N_g (b) $\langle N_g \rangle$ on N_b and (c) $\langle N_S \rangle$ on N_h are depicted in Figs. 4 (a–c). Customarily, the experimental results are analyzed by using the linear fit of the following type:

$$Y = A + B_1 X .$$

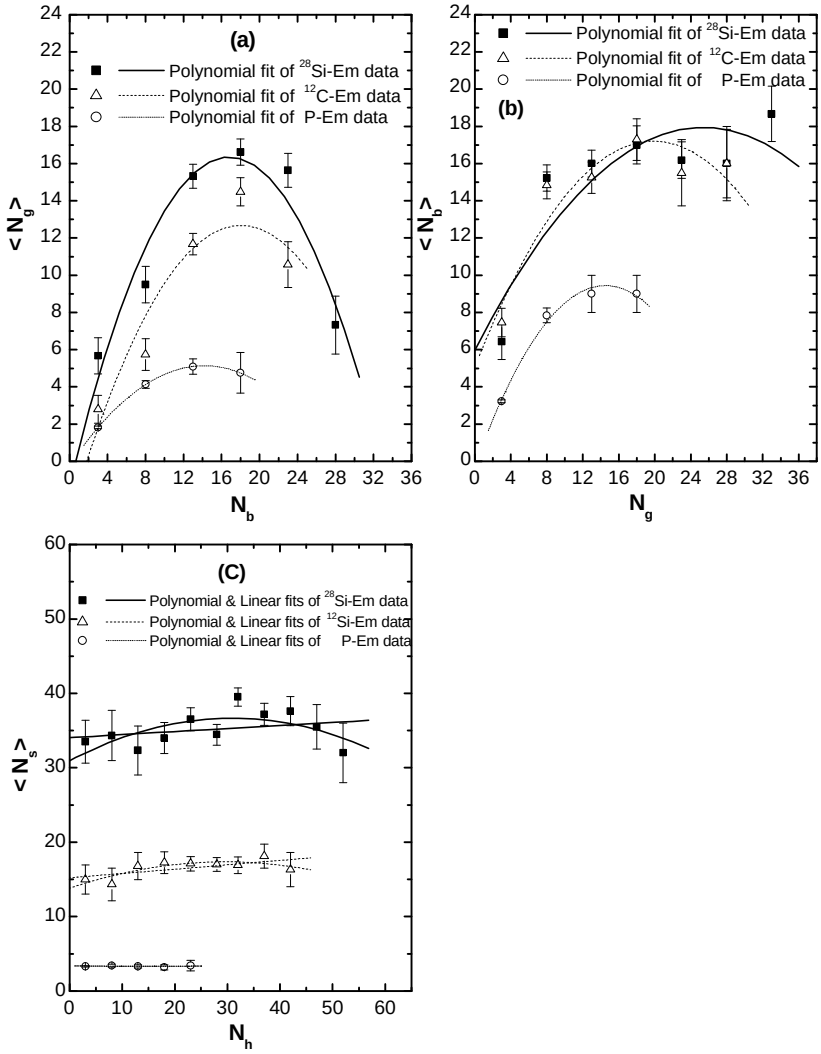

Fig. 4 – Plots for ^{28}Si-Em, ^{12}C-Em and P-Em interactions at 4.5A GeV/c: a) $\langle N_g \rangle$ *vs.* N_b; b) $\langle N_b \rangle$ *vs.* N_g (c) $\langle N_S \rangle$ *vs.* N_h and also their respective linear and polynomial regressions.

These figures suggest that whereas the linear regressions are feasible only for $<N_S>$ *vs.* N_h correlations and not that for other inter-correlations under consideration. Thus, we tried to fit the polynomial regressions of second order, i.e.,

$$Y = A + B_1 X + B_2 X^2;$$

just to see the magnitude of the departure/deviation present if any, from the linear regression in these regressions, viz., $<N_b>$ *vs.* N_g and $<N_g>$ *vs.* N_b plots . The values of the fitted parameters are listed in Table 2. The used parameters A, B_1, B_2, R-Square, SD and P are usual statistical regression coefficients and detail may be found in Appendix.

Table 2

Values of the fitted parameters A, B_1 and B_2 of the equation $Y = A + B_1X + B_2X^2$; along with other related parameters for ^{28}Si-Em, ^{12}C-Em and P-Em interactions at 4.5A GeV/c

Interactions	Correlations	A	B_1	B_2	R-Square	SD	P
^{28}Si-Em	$<N_s>$ *vs.* N_h	30.945±1.914	0.370±0.160	-0.005±0.003	0.411	1.995	0.120
($N_S \geq 28$)		34.051±1.454	0.041±0.046	**0***	0.282	2.352	0.401
	$<N_g>$ *vs.* N_b	-2.978±3.437	1.736±0.621	-0.048±0.023	0.893	2.177	0.107
	$<N_b>$ *vs.* N_g	5.966±3.023	0.944±0.390	-0.019±0.011	0.752	2.419	0.062
^{12}C-Em	$<N_s>$ *vs.* N_h	13.824±0.821	0.240±0.085	-0.004±0.002	0.684	0.765	0.032
($N_S \geq 14$)		15.227±0.657	0.058±0.025	**0***	0.654	0.953	0.056
	$<N_g>$ *vs.* N_b	-1.302±2.513	2.105±0.379	-0.063±0.119	0.912	1.816	0.026
	$<N_b>$ *vs.* N_g	5.088±2.228	1.223±0.336	-0.031±0.011	0.873	1.610	0.045
Proton-Em	$<N_s>$ *vs.* N_h	3.426±0.192	-0.017 ±0.035	0.001±0.001	0.106	0.122	0.894
($N_S \geq 3$)		3.351±0.098	-0.0004±0.007	**0***	-0.035	0.105	0.956
	$<N_g>$ *vs.* N_b	-0.204±0.021	0.756±0.005	-0.027±0.0002	1.000	0.011	0.004
	$<N_b>$ *vs.* N_g	-0.253±0.975	1.338±0.220	-0.046±0.010	0.988	0.512	0.108

- $B_2 = 0^*$ corresponds to the linear regression: $Y = A + BX$

The following conclusions may be drawn from theses graphs and the table:

(i) Dependence of $<N_S>$ on N_h: It is observed that $<N_S>$ remains same for all values of N_h in the case of Proton-Em data and fitted with linear regression. However, ^{28}Si-Em and ^{12}C-Em data are fitted to polynomial regression of second order which depict small deviations from linearity. The careful study of regression coefficients, R-square clearly indicates that the observed mild departure from the linearity is attributed to the correlations which are basically linear with some saturations at high values of N_h. The projectile mass dependence is also observed.

(ii) Variation of $<N_b>$ with N_g: Initially, the value of $<N_b>$ increases almost linearly to a maximum value and then decreases rapidly for the higher values of N_g.

(iii) $<N_g>$ as a function of N_b: A similar trend as observed in the case of $<N_b>$– N_g correlations may also be seen here along with marked projectile mass dependence.

(iv) The $<N_b>$ – N_g and $<N_g>$ – N_b correlations are almost perfectly positively correlated as the values of R-square are estimated and listed in the Table 2 to be ~ 1.

(v) The large values of P (~ 0.05) in the table suggest that the goodness of the fit is satisfactory.

4.4. ANGULAR DISTRIBUTIONS OF TARGET FRAGMENTS AND SHOWER PARTICLES

The angular distribution of target fragments, i.e., grey and black tracks are plotted in Figs. 5 (a, b) and 6 (a, b) respectively. No peculiarity in the plots is observed which may indicates the occurrence of any abnormal phenomena. The front ($\theta < 90^{\circ}$) to back ($\theta > 90^{\circ}$) F/B ratio and the average values of the median angles, $\theta_{1/2}$ (the angle in which fly half of all the particles) for these distributions are listed in Table 3. A weak dependence of the above parameters suggests the mild enhancement in the collision impact with increasing mass of projectiles.

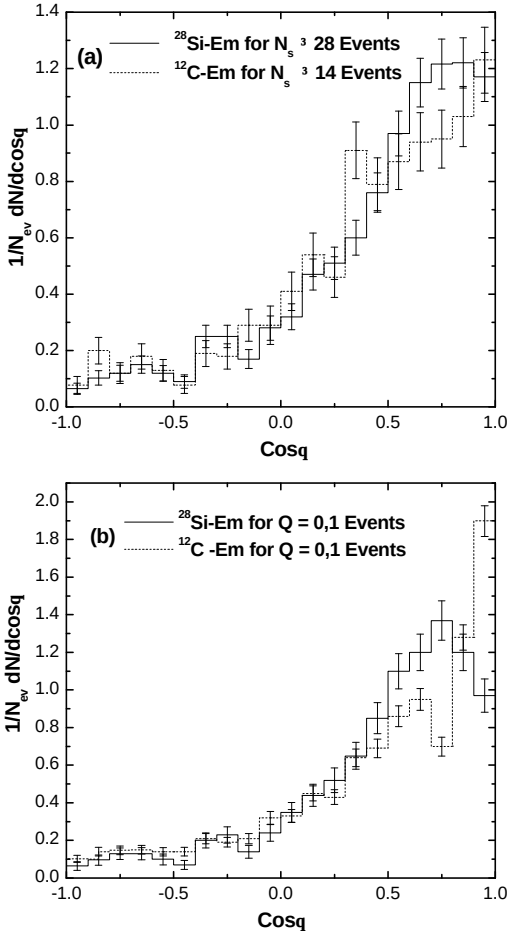

Fig. 5 – Angular distributions of grey tracks for ^{28}Si-Em and ^{12}C-Em interactions at 4.5A GeV/c: a) for $N_s \geq 28$ and $N_s \geq 14$ events; b) for $Q = 0,1$ events.

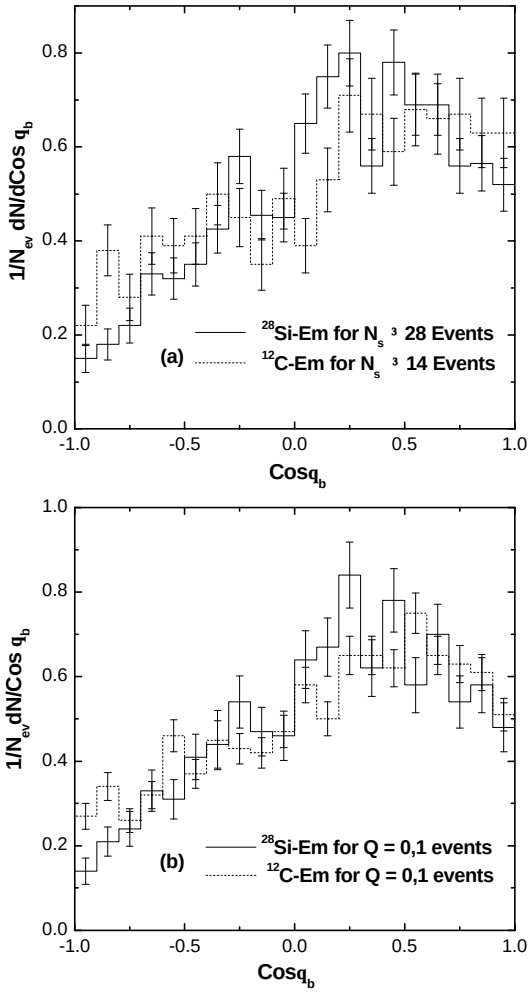

Fig.6 – Angular distributions of black tracks for ^{28}Si-Em and ^{12}C-Em interactions at 4.5A GeV/c: a) for $N_s \geq 28$ and $N_s \geq 14$ events; b) for $Q = 0,1$ events.

Table 3

Values of F/B ratio and $\theta_{1/2}$ for angular distribution of the produced particles in nuclear collisions at 4.5A GeV/c

F/B and ?$_{1/2}$				
Beam	Momentum (A GeV/c)	Grey	Black	Sample
Silicon	4.5	5.23 ± 0.36 56.6°	1.91 ± 0.099 78.5°	$N_S \geq 28$
		5.90 ± 0.47 58.3°	1.82 ± 0.100 81.4°	$Q = 0,1$

Table 3 (continued)

Carbon	4.5	4.35 ± 0.37 60.0° 4.66 ± 0.23 59.5°	1.61 ± 0.097 75.5° 1.61 ± 0.058 82.0°	$N_S \geq 14$ $Q = 0{,}1$

The normalized pseudorapidity distributions, $\frac{1}{N_{evt}} \frac{\mathrm{d}n}{\mathrm{d}\eta}$, (i.e., the particle number densities in rapidity space) of the secondary charged shower particles emitted in ^{28}Si-Em and ^{12}C-Em interaction at 4.5A GeV/c for both the ensembles have been shown in Fig.7 (a, b). The distributions are normalized for total number of interactions in each sample. From these figures we may notice that the plots are

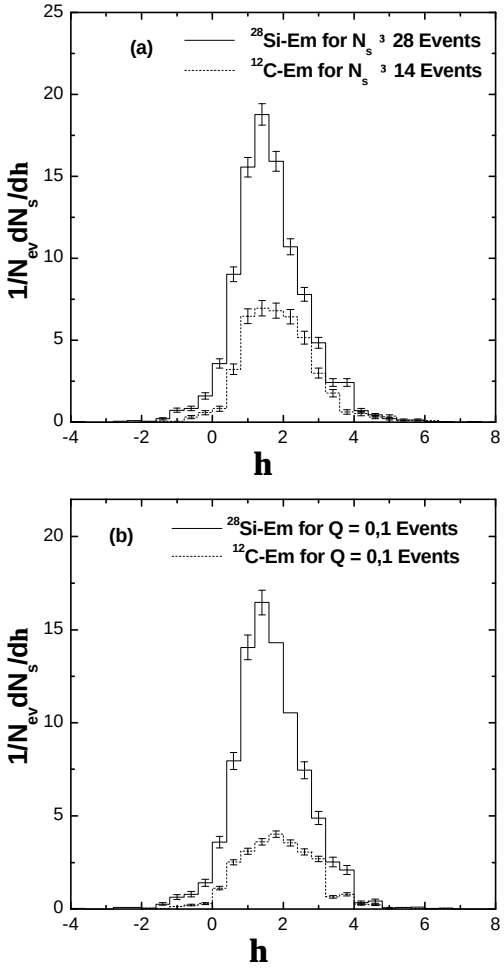

Fig. 7 – Pseudorapidity distributions of shower particles for ^{28}Si-Em and ^{12}C-Em interactions at 4.5A GeV/c: a) for $N_s \geq 28$ and $N_s \geq 14$ events; b) for $Q = 0.1$ events.

essentially similar and no scaling either in the projectile fragmentation region (i.e., higher values of η) or in the target fragmentation region (i.e., lower values of η) is observed, which indicates that the entire rapidity range is available for the multiparticle production. The heights and widths of the distribution increase with increase in the projectile mass and energy. The height of the centroid increases many times in the case of ^{28}Si-Em collisions with respect to the ^{12}C-Em interactions, which could be explained using the geometry of the collision as increase in the degree of centrality.

5. CONCLUSIONS

The study of the high N_S-multiplicity events, criteria selecting for central collisions in the interactions of $^{25.8}$Si-Em, ^{12}C-Em and Proton-Em at the energy 4.5A GeV/c allows us to draw the following conclusions:

(i) In the events of total destruction of nuclei, the entire rapidity range is available for the production of particles in nucleus-nucleus collisions and effects of both projectile and target fragmentations are eliminated.

(ii) The observed features may be understood in terms of geometry of the collision.

(iii) A weak dependence in the values of the forward to backward (F/B) ratio and $\theta_{1/2}$ clearly indicates the mild enhancement in the collision impact with increasing mass of the projectiles.

(iv) The criteria for selection of central collision events adopted in the study based on multiplicity of charged shower particle (N_S) seems to be equally good like other criteria used by other investigators [15, 17]. However, it is not applicable for Proton-Em data.

Acknowledgement: The financial assistance provided to M. Tariq working as Reader in the Department of Physics at Govt. Raza P. G. College, Rampur (U.P.) India for undertaking Minor Research Project, No: F. 5.1.3 (Phy) 20/05 (MRP/NRCB) by University Grant Commission, New Delhi India is highly acknowledged.

APPENDIX

Correlation. Whenever two variables x and y are so related such that a change in one is accompanied by the change in the other in such a way that an increase (or decrease) in one is accompanied by an increase or decrease (or decrease or increase), in the other, then the variables are said to be correlated.

Regression. The term “regression” was first used by a British Biometrician Sir Francis Galton (1822-1911) in the later part of nineteenth century and profound the “Law of Universal Regression”. The dictionary meaning of regression is

"stepping back". But now-a-days the term 'regression' stands for some sort of functional relationship between two or more related variables. Moreover, the only fundamental difference between the problems of curve fitting and regression, if any, is that in regression any of the variable may be considered as independent or dependent, while in curve fitting one variable can not be dependent. For example, in a time series, the time does not depend on any variable, but the variables depend on time.

Nevertheless it is true in the sense that the study of the interdependence leads to the theory of correlation, while the study of the dependence leads to the theory of regression. However, in the present study correlations and regressions are assumed some what similar and the properties of various regression coefficients have been utilized. They are the correlation coefficient *R*-Square, the standard deviation *SD*, *P*-values (the probability that *R*-Square is zero), etc. Some observed features about *R* are as under:

1. If $R = +1$ or -1, the two regression lines will coincide. The variables are perfectly correlated. If $R = -1$, the variables are perfectly negatively correlated, low values of one corresponding to high values of the other. If $R = +1$, variables are perfectly positively correlated, high values of one corresponding to high values of the other.
2. If $R = 0$, the two lines of regression become $X = M_x$ and $Y = M_y$ which are two lines parallel to *Y* and *X* axes, passing through their means M_x and M_y. They are perpendicular to each other. It means that mean values of *X* and *Y* do not change with *Y* and *X* respectively, i.e., *X* and *Y* are independent.
3. Following are the diagrams for various values of *R*:

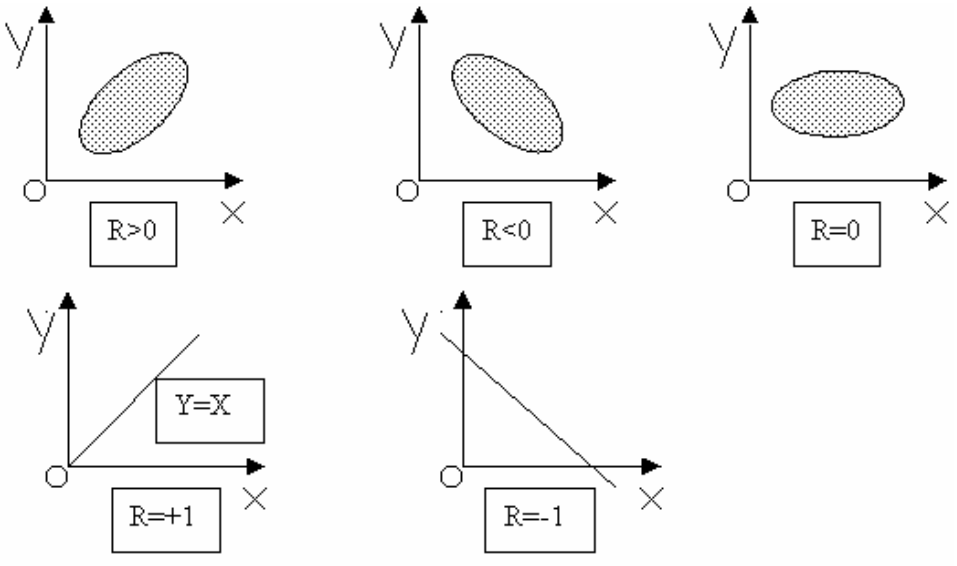

REFERENCES

1. M. Gazdzicki and S. Mrowczynski. Z. Phys., **C54,** 127 (1992).
2. S. Mrowczynski, Phys.Lett., **B439**, 6 (1998).
3. M.A. Halasz, A. D. Jackson, R.E. Shrock, M.A. Stephanev and J.J.M. Verbaarschot, Phys. Rev., **D58**, 96007 (1998).
4. M. Tariq, S. Ahmad, A. Tufail and M. Zafar, Nuovo Cim., **A107**, 2687 (1994).
5. N.N. Abd-Allah, S.A.H. Abou-Steit, M. Mohery and S.S. Abdel Aziz, Int. J. Mod. Phys., **E10**, 55 (2001).
6. A-ABDDKLMTU-B Collaboration, Z. Phys., **A302**, 133 (1981).
7. M. Tariq, M. Zafar and S. Ahmad, Int. J. Mod. Phys., **E1**, 859 (1992).
8. M. Tariq, A. Tufail, S. Ahmad and M. Zafar, Nuovo Cim., **A106**, 617 (1993).
9. Shafiq Ahmad, M. Ayaz Ahmad, M. Irfan and M. Zafar, J. of the Physical Society of Japan, **75**, 6, 064604 (2006).
10. M. Tariq, M. Zafar, A. Tufail and S. Ahmad, Int. J. Mod. Phys., **E4**, 347 (1995); M. Q.R. Khan, M. S. Ahmad, K. A. Siddiqui and R. Hasan, Nuovo Cim., **99A**, 417 (1988); A. El-Naghy and V. D. Toneev, Z. Phys., **A298**, 55 (1980); M. I. Adomovich *et al.*, **E1-10838**, Prep. JINR Dubna, 1977.
11. K.D. Tolstoy, Z. Phys., **A301**, 339 (1981); Tauseef Ahmad, M. Tariq, M. Irfan, M. Zafar, M. Z. Ahsan and M. Shafi, Can. J. Phys., **67**, 519 (1989); A. Abduzhamilov *et al.*, Phys. Rev.**, D39**, 86 (1989).
12. Barashenkov *et al.*, Nucl. Phys., **14**, 522 (1959).
13. B. Jokobsson and R. Kullburg Phys. Scr., **13**, 327 (1976).
14. A.El-Naghy Nouvo Cim.**, 71**, 245 (1982); M. El-Nadi, A.T. Baranik, A. El-Naghy, N. Mettwalli, O.E. Badawy and S. Abd EL-Halim, Z. Phys.**, A310**, 301 (1983); L.M. Barbier *et al.*, Phys. Rev. Lett., **60**, 405 (1988); Fu-Hu-Liu, Chinese J. Phys., **40**, 159 (2002).
15. Prithipal Singh, M. Saleem Khan and H. Khushnood, Can J. Phys.**, 76**, 559 (1998); N. N. Abd-Allah, Can J. Phys., **78**, 915 (2000).
16. El-Nadi *et al.*, J. Phys., **G19**, (2027, 1993) and **G24**, 2265 (1998).
17. M.El-Nadi *et al.*, Eur. Phys. J.**, A10**, 177 (2001).